Investigation of CdS Photoanode Reaction in the Electrolyte Solution Containing Sulfide Ion

Tooru INOUE,* Tadashi WATANABE, Akira FUJISHIMA, and Kenichi HONDA

Department of Synthetic Chemistry, Faculty of Engineering, The University of Tokyo, Hongo, Bunkyo-ku, Tokyo 113

(Received July 19, 1978)

The study of the photoanodic reaction in the CdS/S^{2-} system was carried out by means of the rotating ring-disk electrode (RRDE) technique. The photoanodic reactions at an n-type CdS electrode are divided into two types; the photoanodic oxidation of redox agents in the electrolyte solution and the photoanodic dissolution of CdS electrode surface. The stabilization of a CdS photoanode could be attained through the preferential progress of the former of these two processes. The ratio between these two processes depends upon the concentration of S^{2-} in the electrolyte solution and the light intensity. Sulfide ion in the electrolyte solution stabilizes CdS photoanode and gives rise to the shift of the flatband potential of CdS electrode by *ca.* -60 mV/log[S^{2-}]. This dependence of the flatband potential on sulfide ions can be explained by an adsorptive dissociation equilibrium at a CdS electrode surface. The results of the photoanodic reaction were disscussed referring to the charge transfer process with the participation of some surface energy state within a bandgap.

The behavior of the reactions at an illuminated semiconductor electrode has been recently drawing attention of a number of investigators primarily in connection with the solar energy conversion into electrical and chemical energy, that is, the electrochemical photocell as a solar energy converting device.[1-24]

At TiO_2 electrode[1-10] and other stable semiconductor electrodes,[11-14] the photosensitized electrolytic oxidation of water[1-14] and various reducing agents such as I^-, Br^-, Cl^-, $Fe(CN)_6^{4-}$, hydroquinone, and Fe^{2+} [15-25] occurs by the action of the excess holes photogenerated at the electrode surface, according to the following reactions.

$$2H_2O + 4h^+ \longrightarrow O_2 + 4H^+ \quad (1)$$

$$Red + n\,h^+ \longrightarrow Ox \quad (2)$$

These semiconductors possess relatively wide bandgaps except WO_3[8] and Fe_2O_3[4,13] and hence can not efficiently utilize the solar energy. In this respect, cadmium sulfide[15-21] seems to be a promising material since it shows a strong absorption in wavelength shorter than 520 nm. However, the anodic reaction at an illuminated CdS electrode is known to be the dissolution[26,27] of the electrode surface, according to

$$CdS + h\nu \longrightarrow CdS(h^+_{val} + e^-_{cond}), \quad (3)$$

$$2h^+_{val} + CdS \longrightarrow S_{ad} + Cd^{2+}, \quad (4)$$

where h^+_{val}, e^-_{cond} and S_{ad} denote a hole in the valence band, an electron in the conduction band, and a sulfur atom deposited on the electrode surface, respectively.

Hence, from the stand-point of practical application of CdS photoanode to the electrochemical photocell, it is desired to stabilize the CdS photoanode. In the previous paper[15] we investigated the suppression of surface dissolution of CdS photoanode by reducing agents through the competitive oxidation between the process (2) and (4).

Some reducing agents had the various efficiencies of the dissolution suppression and especially S^{2-}, SO_3^{2-}, and $S_2O_3^{2-}$ could markedly stabilize the CdS photoanode.[15] Wrighton *et al.*[19] reported that the cadmium calcogenide (CdX) photoanodes are stabilized through the oxidation of the calcogenide ions (S^{2-}, Se^{2-}, and Te^{2-}) in the electrolyte solution and the output power characteristics of the electrochemical photocell can be enhanced by using the CdX/X^{2-} systems.

Miller and Heller[21] also reported the power characteristics of the photocells with CdS and Bi_2S_3 polycrystal photoanodes/sulfide. Minoura *et al.*[16] reported that the dissolved Cd^{2+} and S^{2-} ions cause the shift of the flatband potential of CdS and CdS photoanode is stabilized by the diffusion of S^{2-} to the electrode surface. Memming[20] investigated the oxidation efficiency of a ferrous cyanide at the CdS photoanode surface against pH variation by means of a rotating platinum-semiconductor RRDE technique.

As for the effect of the illumination intensity on the electrochemical photolysis of water at TiO_2 and on the conversion of the light energy to the electricity at CdS, the power charateristics (photovoltages and photocurrents) of the electrochemical photocells were investigated well.[19,28] However, a quantitative dependence of the light intensity on the stability of CdS photoanode has not been investigated in detail.

In this study,[45] we investigated more precisely the dependence of a flat band potential on the dissolved sulfide ion and the dependence of the competitive reaction between the dissolution of CdS photoanode and the oxidation of the dissolved sulfide ions on the light intensity by means of a RRDE technique and others. We show the results that the stabilization of the CdS photoanode can be elucidated based upon the function of the concentration of the sulfide ions and the number of the incident photons. Then we discussed the charge transfer across the semiconductor/electrolyte interface based upon the number of the carriers in both phases.

Experimental

Ring-disk electrode were constructed with single crystal of n-type CdS disk electrode together with Cu(Hg) as the ring electrode. General experimental procedures including electrode pretreatments, establishment of ohmic contacts and RRDE assembly have described elsewhere.[15,29]

The measurement principle of the RRDE method is schematically illustrated in Fig. 1. In the absence of a reducing agent (S^{2-}) in the electrolyte solution (A), Cd^{2+} ion is pro-

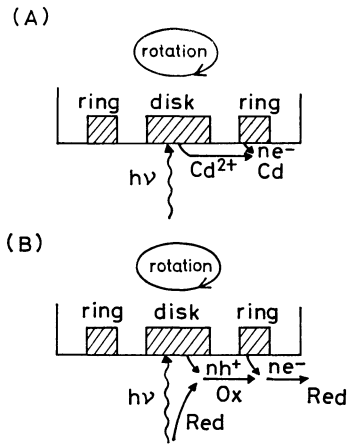

Fig. 1. Schematic diagram of the RRDE system. (A) a detection of the dissolution product of CdS electrode surface, (B) a detection of the oxidation product of a reducing agent.

duced at the disk electrode through the photoelectrochemical process (4), and a part of which, determined by the collection efficiency, is reduced at the Cu(Hg) ring electrode. If a reducing agent is added (B), it undergoes the competitive oxidation of S^{2-} by photogenerated holes, and the oxidized species discharges at the ring electrode.

Dependence of the flatband potential of CdS photoanode on the concentration of the sulfide ion was given by the capacitance measurement of the interface of CdS electrode/electrolyte solution containing sulfide ion, whose method is described in elewhere.[30]

Results and Discussion

Variation of Flatband Potential of CdS Electrode. Figure 2 shows typical $1/C^2$ *vs.* E plots for the CdS electrode in the aqueous electrolyte solution with sulfide ions, obtained by the impedance measurement. The interface capacitance is assumed that the capacitance of a space charge layer is much smaller than any other regions. When a depletion layer is formed for majority carriers (electrons) for n-type semiconductor such a condition can be attained at the anodic polarization. So the determination of the flatband potential of CdS

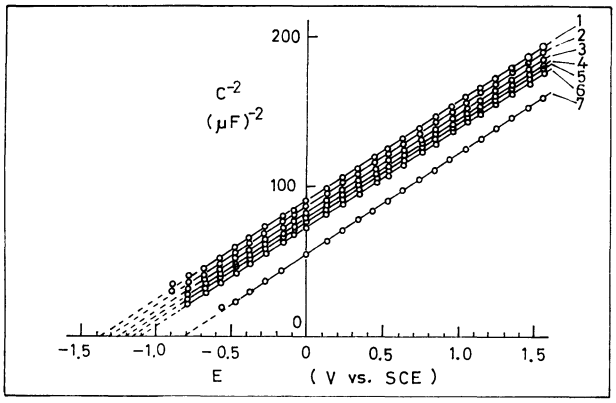

Fig. 2. Mott-Schottky plots for CdS electrode. 1: 1.0 M S^{2-}, 2: 10^{-2} M S^{2-}, 3: 10^{-2} M S^{2-}, 4: 10^{-3} M S^{2-}, 5: 10^{-4} M S^{2-}, 6: 10^{-5} M S^{2-}, 7: 0.0 M S^{2-}. All in 0.2 M Na_2SO_4 aqueous solution.

electrode is based upon the application of Mott-Schottky relationship[31] which is expressed as

$$\frac{1}{C_s^2} = \frac{2}{qee_0N}\left(E - E_{fb} - \frac{kT}{q}\right), \tag{5}$$

where C_s represents the space charge differential capacitance per unit area, q the electric charge, e the dielectric constant of semiconductor, e_0 the permittivity of vacuum, N the carrier concentration (practically equals the donor concentration in the present case (7.4×10^{16} cm^{-3})), E the electrode potential and E_{fb} the flatband potential. Thus the intercept of the E axis of the $1/C^2$ (approximately equals $1/C_s^2$) *vs.* E curves gives a potential differing from the flatband potential by kT/q.

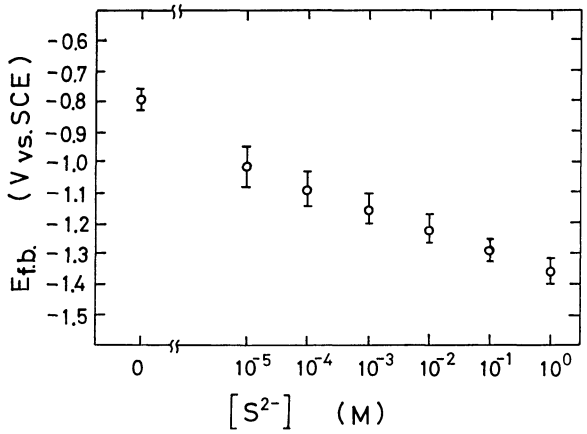

Fig. 3. Dependence of the flatband potential of CdS electrode on the concentration of S^{2-}.

The flatband potentials of CdS electrode thus determined is shown in Fig. 3 as a function of the concentration of S^{2-} with the slope *ca.* -60 mV/log[S^{2-}]. The value of this slope is approximately the same as that reported by others.[32] Otherwise, the flatband potentials of TiO_2 and ZnO depend upon the pH of the electrolyte solution with a slope of -59 mV/pH, which is explained in view of the following dissociation equilibrium established at the semiconductor electrode surface,[33] for example

$$\text{Ti-O}^{2-} + \text{H}^+ \rightleftharpoons \text{Ti-OH}^-, \tag{6}$$

$$\Delta\phi = \text{const} + \frac{RT}{E}\ln\frac{a_{\text{TiO}^{2-}}}{a_{\text{TiOH}^-}} - \frac{2.3RT}{F}\text{pH},$$

where Ti–O^{2-} represents an element of the TiO_2 lattice at the surface, H^+ a proton in the bulk of the electrolyte solution, and Ti–OH^- the lattice element protonated. From the thermodynamic theory, the flatband potential is reasoned with the inner potential difference of the interface between the electrode surface and the electrolyte solution. In the case of CdS electrode in the present study, the same consideration may well be taken.

$$\begin{matrix}-\text{Cd}_L^{\delta+} \\ -\text{Cd}_L^{\delta+}\end{matrix} + S_{soln}^{2-} \rightleftharpoons \begin{matrix}-\text{Cd}_L^{(\delta-1)+} \\ -\text{Cd}_L^{(\delta-1)+}\end{matrix}\rangle S_{ad} \tag{8}$$

where $-Cd_L^{\delta+}$ represents the lattice cadmium element of the CdS lattice at the surface, S_{soln}^{2-} a sulfide ion in

the electrolyte solution, $-Cd_L^{(\delta-1)+}\rangle S_{ad}$ the lattice cadmium element adsorbed by a sulfide ion. That is, the interfacial potential difference ($\Delta\phi$) generated by a surface adsorptive dissociation equilibrium of a sulfide ion at the CdS electrode surface depends upon the concentration of the sulfide ion in the bulk of the electrolyte solution and then changes the flatband potential of CdS electrode according to the following equation[34]

$$E_{fb} \simeq \Delta\phi = \text{const} - \frac{RT}{F}\ln\frac{C(N^\circ - N)}{C^\circ N}, \quad (9)$$

where N° and N represent the surface concentrations of adsorbed sulfide ions for maximal coverage and for the equilibrium state, C and C° the concentration of sulfide ions in solution and that in the standard state.

Consequently, the fact that the flatband potential of CdS photoanode shifts to the negative potential implies that the power characteristics, especially the photo-output voltage, of an electrochemical photocell can be increased, because the onset potential of the photocurrent based upon a photoanodic reaction corresponds to the flatband potential of a photoanode.

Current-potential Characteristics of Cu(Hg)/CdS RRDE. An anomalous behavior of the CdS disk photocurrent was observed uniquely on addition of S^{2-} in the electrolyte solution. Figure 4 shows the change of the current-potential characteristics of CdS photoanode with the change in S^{2-} concentration. It is seen that the onset potential for the photocurrent is shifted to more negative potential as S^{2-} concentration increases, corresponding to the flatband potential in Fig. 3, and the photocurrent appears as the twostep wave in lower S^{2-} concentrations. In the dark, the anodic photocurrent does not appear, but under illumination the anodic photocurrents appear at the negative onset potentials. In the absence of the sulfide ion in the electrolyte solution, the limiting anodic photocurrent is controlled by the photogenerated holes at the electrode surface. On the other hand, the first wave of the photocurrent observed in a lower concentration of S^{2-} increases with an increase in the concentration of S^{2-} in the electrolyte solution. In a high concentration of S^{2-}, the photoanodic current becomes one-step wave again. This phenomenon of appearance of a two-step wave photocurrent is considered to be originated from two different reactions at CdS electrode. Minoura and Tsuiki have also reported two- or three-step wave photocurrent in the solution containing S^{2-}, SO_3^{2-}, and $S_2O_3^{2-}$.[35,36] In TiO_2 electrode, a two-step wave photocurrent, it is reported,[37] appears at high pH values of the electrolyte solution, and it is explained that the first wave photocurrent is controlled by the diffusion of a hydroxyl ion (OH^-) to the TiO_2 surface and the second one by that of water (H_2O).

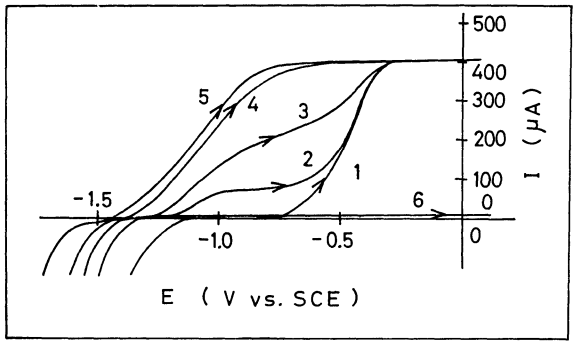

Fig. 4. Current-potential curves of a rotating CdS electrode at 1000 rpm in the electrolyte solution containing various concentrations of S^{2-}.
1: 0.0 M S^{2-}, 2: 7×10^{-4} M S^{2-}, 3: 10^{-3} M S^{2-}, 4: 10^{-2} M S^{2-}, 5: 10^{-1} M S^{2-}, above 1—5; at illuminated, 6: in the dark. All in 0.2 M Na_2SO_4 solution.

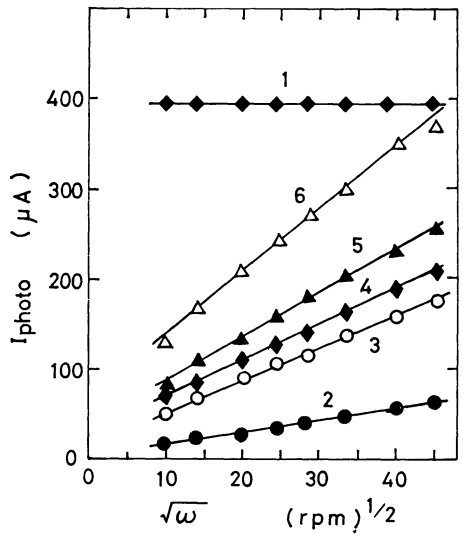

Fig. 5. Dependence of photocurrents on the root of a rotating speed of CdS disk electrode.
1: With and without S^{2-}, potentials at 0.0 V (*vs.* SCE), 2: 10^{-4} M S^{2-}, at −0.8 V, 3: 5×10^{-4} M S^{2-}, at −0.8 V, 4: 7×10^{-4} M S^{2-}, at −0.8 V. 5: 10^{-3} M S^{2-}, at −0.8 V, 6: 1.5×10^{-3} M S^{2-}, at −0.8 V. All in 0.2 M Na_2SO_4 solution.

Concerning the appearance of the two-step wave of an anodic photocurrent, the dependence of the first and the second waves on the rotation speed (ω) was measured and the results are illustrated in Fig. 5. The magnitude of the second wave shows practically no change with ω, which means that the rate-determining step is the formation of photoholes in the valence band. On the contrary, the magnitude, I_{photo}, of the first wave varies linearly with the square root of ω, and increases in an increase of S^{2-} concentration. I_{photo} can be approximated by the following formula,

$$I_{photo} = \text{const} \times [S^{2-}]\omega^{1/2} \quad (10)$$

which, according to the theory of Levich,[38] indicates that the process corresponding to the first wave is controlled by the diffusion of S^{2-} from the solution to the CdS electrode surface. Therefore, the first wave photocurrent is considered to occur from the following reactions

$$nS^{2-} + 2(n-1)h^+ \longrightarrow S_n^{2-} \quad (n=2, 3, 4, 5), \quad (11)$$

or

$$S^{2-} + 2h^+ \longrightarrow S,$$
$$S + S^{2-} \longrightarrow S_2^{2-}. \quad (12)$$

This photoanodic oxidation at CdS photoanode was also reported by Wrighton *et al.*[19] Miller and Heller,[21] and Minoura *et al.*[16]

Figure 6 shows the dependence of the disk (I_D) and ring (I_R) currents on the ring potential (E_R), with or without S^{2-} added in the electrolyte solution. In the dark (curves 1, 3), negligibly small currents are observed at the CdS disk electrode fixed at +1.0 V *vs.* SCE, while hydrogen evolution ($E_R < -1.5$ V) occurs at the Cu(Hg) ring electrode. Illumination of the CdS disk gives rise to an anodic photocurrent (curve 2) and at the same time a reduction current appears at the Cu(Hg) ring electrode in the potential range more negative than −0.6 V *vs.* SCE. The latter current corresponds to the reduction of Cd^{2+} produced by the dissolution reaction of the CdS photoanode (4). Since the ratio of the limiting reduction current at the Cu(Hg) ring electrode to an anodic photocurrent at the CdS disk electrode fairly coincides with the theoretical collection efficiency for the ring-disk electrode employed, it is evident that the process (4) is totally responsible for the anodic photocurrents. By addition of 0.1 M Na_2S in the electrolyte solution, the magnitude of the disk photocurrent undergoes practically no change, while a reduction current of Cd^{2+} disappears and a new ring current (curve 4) appears at potentials more negative than −1.2 V *vs.* SCE, corresponding to the reduction (13) of S_n^{2-} generated by the process (11) or (12).

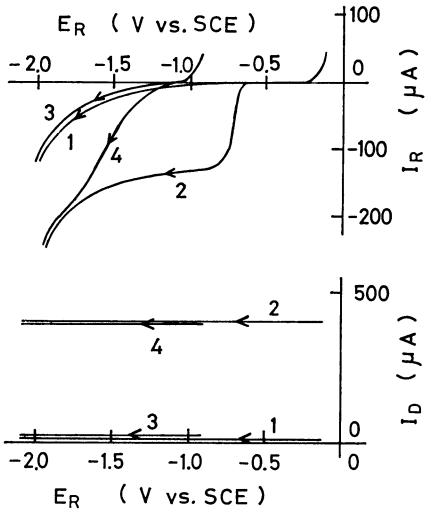

Fig. 6. Current-potential (I_R-E_R, I_D-E_R) curves of Cu(Hg)/CdS RRDE. Potential (E_D) of CdS disk electrode is fixed at 1.0 V vs. SCE.
1: 0.0 M S^{2-}, in the dark, 2: 0.0 M S^{2-}, CdS illuminated 3: 0.1 M S^{2-}, in the dark, 4: 0.1 M S^{2-}, CdS illuminated. All in 0.2 M Na_2SO_4 solution.

$$S_n^{2-} + 2(n-1)e^- \longrightarrow nS^{2-} \quad (13)$$

The occurrence of this process can also be verified by the dependence of the disk and ring currents on the disk potential (E_D), with the ring potential fixed at −1.8 V for S_n^{2-} reduction and at −0.8 to −1.1 V for Cd^{2+} reduction, with or without S^{2-} added in the electrolyte solution, as shown in Fig. 7. In Fig. 7(A), in the absence of S^{2-} in the electrolyte solution both reduction currents (curves 1, 2) at the Cu(Hg) ring electrode are corresponding to the reduction of Cd^{2+}. In Fig. 7(B), in the presence of 5×10^{-4} M S^{2-} added in the electrolyte solution the reduction current (curve 1) at the Cu(Hg) ring electrode appears at the same time in occurance of the second wave of the anodic photocurrent at the CdS disk electrode. Then the reduction current (curve 2) at the ring electrode shows a two-step wave similar to the anodic photocurrent at the CdS disk electrode. This first wave of a reduction current is deduced from the reduction of S_n^{2-}. In Fig. 7(C), in the presence of 0.1 M S^{2-} in the electrolyte solution the reduction (curve 1) of Cd^{2+} at the ring electrode disappears, while the reduction current (curve 2) of S_n^{2-} at the ring electrode shows one wave and its value coincides with the theoretical collection of the disk photocurrent for the ring-disk electrode. Therefore, it is evident that the process (11) or (12) is totally responsible for the anodic photocurrent at the CdS electrode.

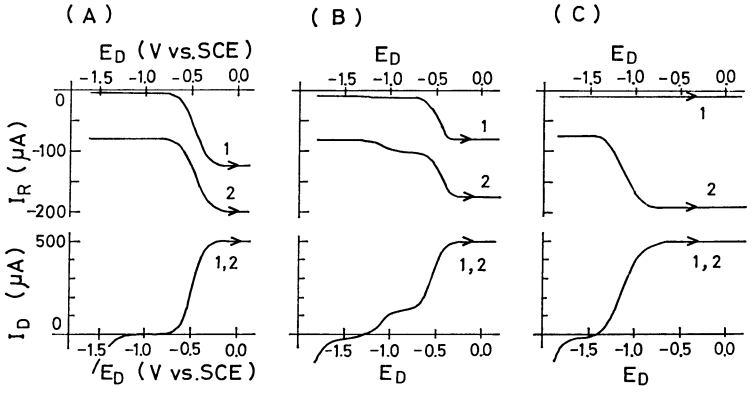

Fig. 7. Current-potential (I_R-E_D, I_D-E_D) curves of Cu(Hg)/CdS RRDE, when CdS disk is illuminated.
(A) With 0.0 M S^{2-}, 1: $E_R = -0.8$ V (*vs.* SCE), 2: $E_R = -1.8$ V. (B) With 5×10^{-4} M S^{2-}, 1: $E_R = -1.0$ V, 2: $E_R = -1.8$ V. (C) With 1×10^{-1} M S^{2-}, 1: $E_R = -1.1$ V, 2: $E_R = -1.8$ V. All in 0.2 M Na_2SO_4 solution.

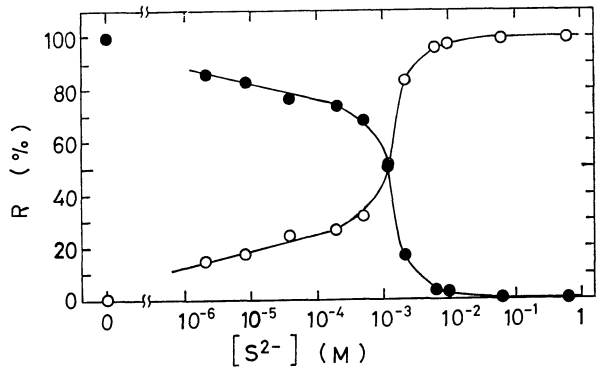

Fig. 8. Dependence of the ratio (R) of a competitive reaction on the concentration of a sulfide ion.
—●—: A dissolution of CdS electrode, —○—: an oxidation of S^{2-} in an electrolyte solution.

If we denote the magnitude of the total ring current by I_R°, that due to Cd^{2+} reduction by $I_{R,Cd}$, and that due to S_n^{2-} reduction by $I_{R,S}$, then $100I_{R,Cd}/I_R^\circ$ and $100I_{R,S}/I_R^\circ$ can be termed as the competition ratio (R) between CdS surface dissolution and oxidation of S^{2-} in the course of the photoelectrochemical process at the CdS photoanode. Figure 8 shows the ratio (R) of the competitive oxidation between CdS photonode and S^{2-} as a function of S^{2-} concentration in the electrolyte solution. It is seen that the value of R for the competitive oxidation of S^{2-} increases with the increase in $[S^{2-}]$ and the value of R for the dissolution of CdS photoanode decreases with the increase in $[S^{2-}]$. This result suggests that in a high concentration of S^{2-} added in the electrolyte solution the dissolution of CdS photoanode can be suppressed, which has been partly reported in a previous paper.[15]

Dependence of Electrode Reactions on Light Intensity. Above results were observed under the constant intensity (*ca.* 3.5×10^{15} photon/s) of illumination (wavelength range from 300 to 410 nm), while the dependence of the two-step wave photocurrent at CdS electrode on the intensity of illumination was observed, as shown in Fig. 9. In Fig. 9(A), with a concentration of 1×10^{-4} M S^{2-} added in the electrolyte solution, in a low intensity of illumination one-step wave photocurrents (curves 1 and 2) appear which are controlled by the number of photoholes formed, and in a high intensity of illumination the two-step wave photocurrents (curves 3 and 4) appear where the first wave photocurrent is constant against the intensity of illumination, however, the second wave photocurrent increases by an increase of the illumination intensity.

In the presence of sufficient sulfide ions in the electrolyte solution, the photocurrent-potential curves become one step waves as shown in Fig. 9(B). In this stage, anodic photocurrents were totally caused by the oxidation of sulfide ions supplied to the CdS electrode surface and the values of photocurrents depend on the number of the incident photons.

The dependence of the two-step wave anodic photocurrents on the intensity of illumination in various concentrations of S^{2-} is shown in Fig. 10. The dots

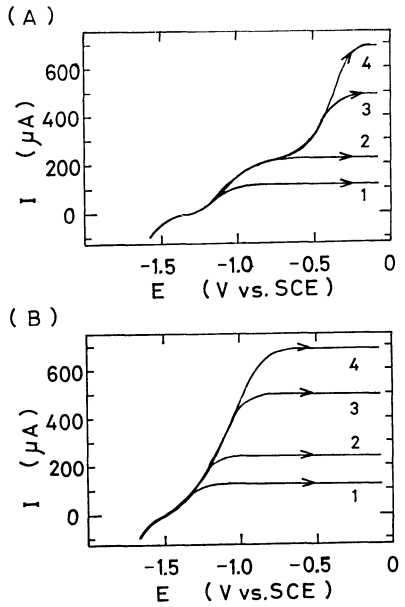

Fig. 9. Dependence of current-potential curves on the intensity (L) of illumination
(A) With 10^{-3} M S^{2-}, 1: L=0.07 a.u., 2: L=0.15, 3: L=0.35, 4: L=0.5. (B) With 10^{-1} M S^{2-}, 1: L=0.07 a.u., 2: L=0.15, 3: L=0.35, 4: L=0.5.

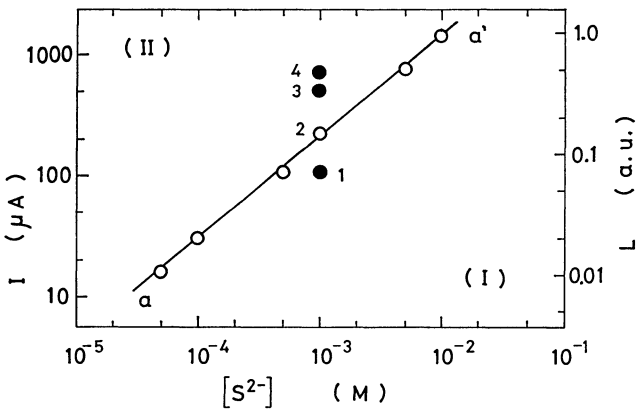

Fig. 10. Dependence of the photocurrents on the illumination intensity (L) and that of the first wave photocurrents on $[S^{2-}]$.

(1, 2, 3, and 4) correspond to the limiting values of the photocurrents in Fig. 9(A), respectively. The curve (a-a') shows the dependence of the limiting photocurrents of the first waves on $[S^{2-}]$. In the region (I) below the curve (a-a'), only a one-step wave photocurrent appears even if the illumination intensity is high, where the oxidation of S^{2-} is controlled by the number of the photogenerated holes. On the contrary, in the region (II) above the curve (a-a'), the second wave photocurrent appears based on the dissolution of CdS photoanode occurs. The oxidation ratio of a sulfide ion depends on the quantitative correlation between the concentration of a sulfide ion and the number of the incident photons.

So we can say that the CdS photoanode can be stabilized when excess sulfide ions are dissolved in the electrolyte solution versus the number of the photo-

TABLE 1. RELATIONS BETWEEN THE THEORETICAL LIMITTING CURRENTS (I_L) AND THE FIRST WAVE-PHOTOCURRENTS (I_P)

$\frac{[S^{2-}]}{mol/l}$	10^{-5}	5×10^{-5}	10^{-4}	5×10^{-4}	10^{-3}	5×10^{-3}	10^{-2}
$\frac{J_L}{mol/s}$	1.80×10^{-11}	8.98×10^{-11}	1.80×10^{-10}	8.98×10^{-10}	1.80×10^{-9}	8.98×10^{-9}	1.80×10^{-8}
$\frac{I_L}{\mu A}$	3.47	17.3	34.7	173	347	1730	3470
$\frac{I_P}{\mu A}$		16.0	29.9	112	211	790	1410
$\frac{[Fe(CN)_6^{4-}]}{mol}$	10^{-5}		10^{-4}		10^{-3}		10^{-2}
$\frac{I_{D,ox}}{\mu A}$	4.0		38.0		310		1760

generated holes at the electrode surface.

Here, we approximate the flow rate (J_L) of the sulfide ion towards the CdS electrode surface and the limiting oxidation current (I_L) of the sulfide ion employing the following equations

$$J_L = 1.95\, D^{2/3}\, \nu^{-1/6}\, \omega^{1/2}[S^{2-}]r^2, \quad (14)$$

$$I_L = nFJ_L, \quad (15)$$

where D denotes the diffusion coefficient, ν the dynamic viscosity, r the radius of the rotating disk electrode, n the covalent number, and F Faraday constant, respectively. Substituting the experimental conditions, $D=10^{-5}$ cm^2/s, $\nu=10^{-2}$ cm^2/s, $\omega=1000$ rpm, $r=0.3$ cm, $n=2$, and $F=96500$, into the Eqs. 14 and 15, we obtain the numerical results for the first-wave photocurrents as shown in Table 1. The oxidation currents($I_{D,ox}$) of varous concentration of $Fe(CN)_6^{4-}$ at the ratating Pt disk electrode with the same diameter as the CdS disk electrode are also shown in Table 1 in order to compare with the magnitude of photocurrents (I_P). From the results of Table 1, we can consider that the first wave photocurrents are controlled almost by the limitting diffusion of sulfide ions and increase with the increase of the sulfide concentration. Reflecting the facts that the flatband potential of CdS and the onset potential of the first wave photocurrent make shifts to the negative potential with the increase of the sulfide concentration, the photogenerated holes may transfer to sulfides *via* the active sites which may be caused by the adsorption of sulfides or by the imperfections (for example, kink sites, step sites or dislocations) on the CdS surface.[39]

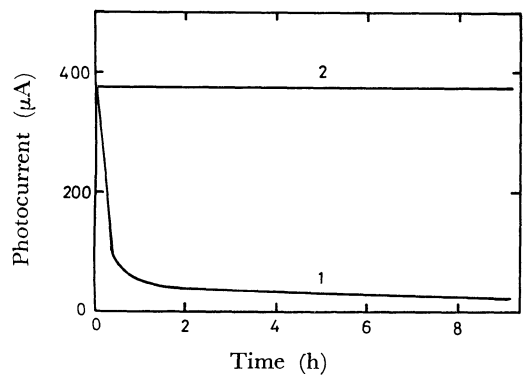

Fig. 11. Time-dependence of photocurrents at CdS electrode. 1: In 0.2 M Na_2SO_4, 2: in 0.2 M Na_2SO_4 +1.0 M Na_2S.

Stabilized CdS Photoanode. From the results in Figs. 8 and 10, we suggest that a stable photocurrent flows at a high concentration of S^{2-} added in the electrolyte solution where the ratio of the competitive oxidation of S^{2-} is almost 100% even if under the high intensity (*ca.* 1×10^{17} photon/cm^2 s) of illumination.

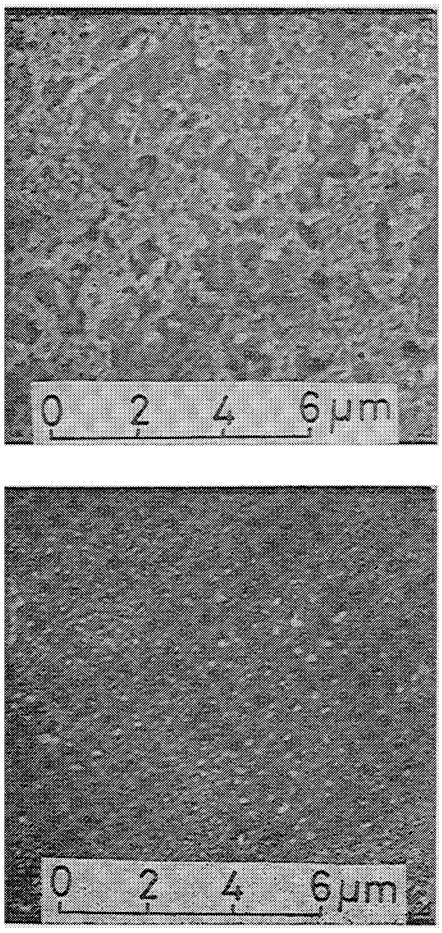

Fig.12. SEM photographs of the CdS electrode surface. (A) After 2 h photoelectrolysis in 0.2 M Na_2SO_4. (B) After 2 h photoelectrolysis in 0.2 M Na_2SO_4+ 0.5 M Na_2S.

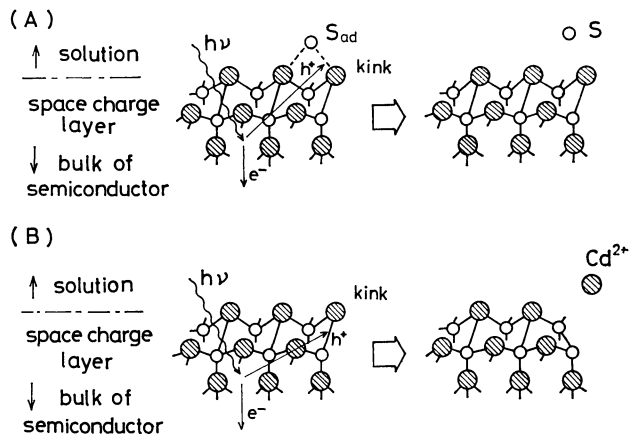

Fig. 13. Schematic diagram of CdS photoanode reactions.
(A) Stabilization of CdS surface with sulfide ions in solution, (B) Oxidation dissolution of CdS surface without sulfide ions in solution.

We show the photocurrent-time characteristics for the electrolyte solution with and without 1.0 M Na_2S in Fig. 11. In the absence of a reducing agent (S^{2-}) in the electrolyte solution, the photocurrent (curve 1) at CdS photoanode usually shows an abrupt decay with time. This phenomenon is attributed to the deposition of sulfur, which acts as a light filter on the electrode surface, produced according to reaction (4). In the presence of a reducing agent (S^{2-}) the photocurrent continues to flow remarkably stably for a long period, as expected above, hence the stabilization of the electrode surface is attained.

The stabilization of CdS photoanode can be visualised by comparing the scanning electron microscopy (SEM) pictures of a CdS surface after photoelectrolysis for 2 hours with (Fig. 12 (B)) and without (Fig. 12(A)) 0.5 M S^{2-} in the electrolyte solution. A rough reticulate structure in (A) might reflect the deposition of sulfur produced by the dissolution reaction (4). The photoanodic reactions at the CdS electrode can be described schematically as shown in Fig. 13, where kink denotes an imperfection site as the example of the active site.

Conclusion

We show in Fig. 14 the schematic diagram of the correlation of the energy levels between a semiconductor (CdS) electrode and reducing agents in the electrolyte solution. E_D in the figure denotes the redox potential of CdS calculated from the thermodynamic data according to the following equation[40]

$$CdS \rightleftharpoons Cd^{2+} + S + 2e^-, \quad E_D = 0.08 \text{ (V } vs. \text{ SCE)}. \quad (14)$$

Concerning the competition ratios[14] of various reducing agents and the values of the reorganization energy (0.7—1.8 eV)[41] of them the charge transfer across the interface is considered to proceed in the participation of some surface energy level.[42]

We propose the schemes in Fig. 15 for the elucidation of the current-potential behaviour of CdS photoanode in contact with an electrolyte solution containing

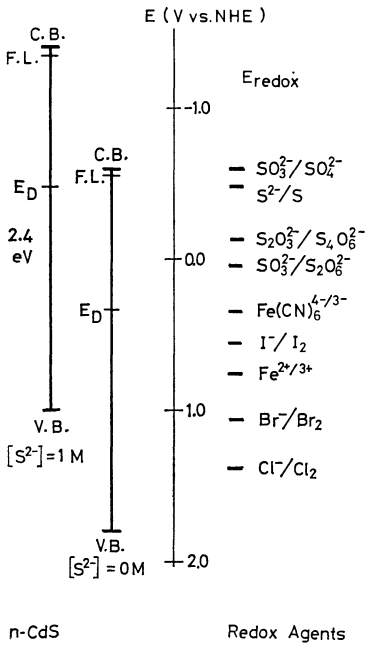

Fig. 14. Schematic diagram of the correlation of the energy levels between a semiconductor (CdS) electrode and reducing agents in the electrolyte solution.

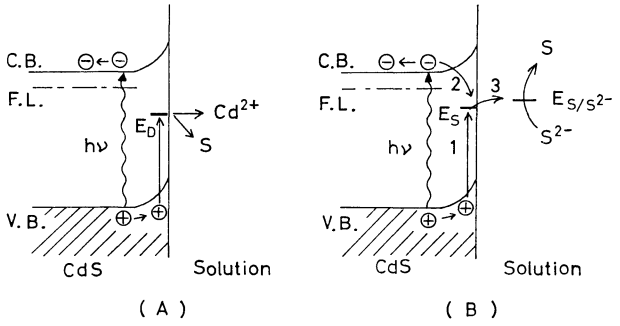

Fig. 15. Schematic diagram of the charge transfer across CdS/electrolyte solution interface.
(A) Dissolution of the CdS electrode surface. (B) Competition between dissolution of the CdS electrode surface and oxidation of S^{2-}.

S^{2-}. Without S^{2-} in solution CdS photoanode can be oxidized by photogenerated holes as shown schematically in Fig. 15(A). In the scheme of Fig. 15(B) it is postulated that a surface state, capable of acting as the recombination center for the photoelectron hole pairs, is induced upon adsorption of S^{2-} on the CdS surface. At potentials differing little from the faltband potential, both the conduction electron (path 2) and hole (path 1) are easily transferred to such a recombination center. A part of the transferred holes, not undergoing recombination, can oxidize S^{2-} by the path 3 at the rate controlled by the diffusion of S^{2-} to the electrode surface (first wave). When the anodic polarization exceeds a critical value, the probability of the path 2 becomes negligible.[43] At this stage, the excess holes begin to oxidize the electrode itself causing dissolution (second wave), since the rate of oxidation of S^{2-} (path 3) is diffusionally controlled. When the electrolyte solution contains excess sulfide

ions against the incident photons the oxidation of a sulfide ion precedes the dissolution of CdS photoanode through the above competitive reaction scheme, which can elucidate the stabilization of the CdS photoanode.[44]

However, the concrete characteristics of the surface state have not been well known, and are currently under investigation in this laboratory.

References

1) A. Fujishima and K. Honda, *Nature*, **238**, 37 (1972).
2) A. Fujishima, K. Kohayakawa, and K. Honda, *J. Electrochem. Soc.*, **122**, 1487 (1975).
3) H. Yoneyama, H. Sakamoto, and H. Tamura, *Electrochem. Acta*, **20**, 341 (1975).
4) K. L. Hardee and A. J. Bard, *J. Electrochem. Soc.*, **123**, 1027 (1976).
5) K. L. Hardee and A. J. Bard, *J. Electrochem. Soc.*, **124**, 215 (1977).
6) A. J. Nozik, *Nature*, **257**, 383 (1975).
7) N. S. Wrighton, D. S. Ginley, P. T. Wolczanski, A. B. Ellis, D. L. Morse, and A. Linz, *Proc. Natl. Acad. Sci. U.S.A.*, **72**, 1518 (1975).
8) G. Hodes, D. Cahen, and J. Manassen, *Nature*, **260**, 312 (1976).
9) J. O'M. Bockris and K. Uosaki, *J. Electrochem. Soc.*, **124**, 98 (1977).
10) R. H. Wilson, *J. Appl. Phys.*, **48**, 4292 (1977).
11) T. Watanabe, A. Fujishima, O. Tatsuoki, and K. Honda, *Bull. Chem. Soc. Jpn.*, **49**, 355 (1976).
12) J. G. Mavroides, J. A. Kafalas, and D. F. Koleser, *Appl. Phys. Lett.*, **28**, 241 (1976).
13) R. K. Quinn, R. D. Nasby, and R. J. Burghman, *Res. Bull.*, **11**, 1011 (1976).
14) Y. Nakato, T. Ohnishi, and H. Tsubomura, *Chem. Lett.*, **1975**, 883.
15) T. Inoue, T. Watanabe, A. Fujishima, K. Honda, and K. Kohayakawa, *J. Electrochem. Soc.*, **124**, 719 (1977).
16) H. Minoura, M. Tsuiki, and T. Oki, *Ber. Bunsenges. Phys. Chem.*, **81**, 588 (1977).
17) H. Morisaki, M. Haraya, and K. Yazawa, *Appl. Phys. Lett.*, **30**, 7 (1977).
18) H. Gerischer and J. Gobrecht, *Ber. Bunsenges. Phys. Chem.*, **80**, 327 (1976).
19) A. B. Ellis, S. W. Kaiser, J. M. Bolts, and M. S. Wrighton, *J. Am. Chem. Soc.*, **99**, 2839 (1977).
20) R. Memming, *Ber. Bunsenges. Phys. Chem.*, **81**, 732 (1977).
21) B. Miller and A. Heller, *Nature*, **262**, 680 (1976).
22) J. Manassen and G. Hodes, *J. Electrochem. Soc.*, **124**, 583 (1977).
23) J. O'M. Bockris and K. Uosaki, *J. Electrochem. Soc.*, **124**, 1348 (1977).
24) H. Tributsch, *Ber. Bunsenges. Phys. Chem.*, **82**, 169 (1978).
25) T. Inoue, T. Watanabe, A. Fujishima, and K. Honda, *Chem. Lett.*, **1977**, 1073.
26) R. Williams, *J. Chem. Phys.*, **32**, 1505 (1960).
27) D. M. Kolb and H. Gerischer, *Electrochem. Acta*, **18**, 987 (1973).
28) J. H. Carey and B. G. Oliver, *Nature*, **259**, 554 (1976).
29) A. Fujishima, E. Sugiyama, and K. Honda, *Bull. Chem. Soc. Jpn.*, **44**, 304 (1971).
30) T. Watanabe, A. Fujishima, and K. Honda, *Chem. Lett.*, **1974**, 897.
31) H. Gerischer, in "Physical Chemistry: An Advanced Treatise," ed by H. Eyring *et al.*, Academic Press, New York (1970). pp. 467—473.
32) H. Minoura, T. Watanabe, T. Oki, and M. Tsuiki, *Jpn. J. Appl. Phys.*, **16**, 865 (1977).
33) A. Fujishima, A. Sakamoto, and K. Honda, *Seisan Kenkyu*, **21**, 450 (1969).
34) H. Gerischer, in "Physical Chemistry: An Advanced Treatise," ed by H. Eyring *et al.*, Academic Press, New York (1970), pp. 473—478.
35) H. Minoura and M. Tsuiki, *Nippon Kagaku Kaishi*, **1977**, 487.
36) H. Minoura and M. Tsuiki, *Electrochem. Acta*, **23**, 1377 (1978).
37) J. L. Desplat, *J. Appl. Phys.*, **47**, 5102 (1976).
38) V. G. Levich, "Physicochemical Hydrodynamics," Prentice-Hall, Englewood Cliffs, N. J. (1962), pp. 60—72.
39) R. H. Wilson, in a private communication and an abstract at the Electrochemical Society meeting in May, 1978.
40) A. J. Bard and M. S. Wrighton, *J. Electrochem. Soc.*, **124**, 1706 (1977).
41) J. M. Hale, in "Reactions of Molecules at Electrodes," ed by N. S. Hush, Wiley-Interscience, London (1971), pp. 229—257.
42) S. N. Frank and A. J. Bard, *J. Am. Chem. Soc.*, **97**, 7427 (1975).
43) P. A. Kohl and A. J. Bard, *J. Am. Chem. Soc.*, **99**, 7531 (1977).
44) A. Fujishima, T. Inoue, T. Watanabe, and K. Honda, *Chem. Lett.*, **1978**, 357.
45) T. Inoue, T. Watanabe, A. Fujishima, and K. Honda, partly presented in "Semiconductor-Liquid Junction Solar Cells: Proceedings of a Conference on the Electrochemistry and Physics of Semiconductor-Liquid Interfaces under Illumination," 77-3, ed by A. Heller, Electrochem. Soc., Princeton (1977), pp. 210—221.